Depth-resolved magnetization profile of MgO/CoFeB/W perpendicular half magnetic tunnel junctions

V. Bansal, J.-M. Tonnerre, E. Mossang, L. Ortega, F. Fettar, J. Chatterjee, S. Auffret, I.-L. Prejbeanu, B. Dieny

Depth-resolved magnetization profile of MgO/CoFeB/W perpendicular half magnetic tunnel junctions

V. Bansal[1*], J.-M. Tonnerre[1,2], E. Mossang[1], L. Ortega[3], F. Fettar[1], J. Chatterjee[4,a)], S. Auffret[4], I.-L. Prejbeanu[4] and B. Dieny[4]

[1]Université Grenoble Alpes, CNRS, Grenoble INP, Institut Néel, 38042 Grenoble, France
[2]Synchrotron SOLEIL, Saint-Aubin, Boite Postale 48, 91192 Gif-sur-Yvette Cedex, France
[3]Université Paris-Saclay, CNRS, Laboratoire de Physique des Solides, 91405, Orsay, France.
[4]University Grenoble Alpes, CEA, CNRS, Grenoble-INP, INAC-SPINTEC, 38000 Grenoble, France
a) Present address: Fraunhofer Institute for Photonic Microsystems, Center for Nanoelectronic Technologies, 01109 Dresden, Germany
* vartika.bansal@neel.cnrs.fr

ABSTRACT

In this work, we used the soft X-ray resonant magnetic reflectivity to study the depth-resolved out-of-plane (*oop*) magnetization profile of a CoFeB/MgO sample with W/Ta cap layer after annealing at 400°C. It is a powerful technique to probe buried magnetic interfaces of ultra-thin films by combining the depth-resolved information of X-ray reflectivity with the species selectivity of X-ray magnetic circular dichroism. It allowed us to resolve the *oop* magnetization within a 1.36 nm thick CoFeB layer by the measurement of angle-dependent specular reflectivity at large scattering angles (up to 80^o). We determined a graded magnetic distribution for both Fe and Co with a 20% increase at the interface with MgO, decreasing slightly over a thickness of 0.7 nm from MgO before it rapidly decreases to 50% at the interface with W. After applying a non-saturating magnetic field in the plane of the sample, we also quantified a similar magnetization profile with an inclined moment configuration. This indicates that the magnetization gradient is a robust property of the CoFeB layer in the studied sample.

I. INTRODUCTION

Magnetic tunnel junctions have been a keen focus in spintronics known for their usage in nonvolatile spin-transfer-torque (STT) magnetic random access memories [1], for which MgO/CoFeB/Ta trilayer systems with perpendicular magnetic anisotropy (PMA) have been proven to be a prime candidate [2]. W insertion between CoFeB and Ta has been shown to improve PMA, thermal robustness and tunnel magnetoresistance (TMR) ratios [3,4]. Moreover, TMR and STT excitation processes are interface-sensitive quantities [5]. Probing magnetic buried interfaces in a layer exhibiting perpendicular magnetization, which limits the thicknesses to the nanometer, is a major challenge. In particular, better understanding of the magnetic interfaces in basic stacks for functional devices can help move beyond the ideal layers and perfect interfaces used for theoretical transport models and understand the difference between predictions and experiments.

In this paper, the magnetization profile of a MgO/CoFeB/W free layer exhibiting PMA after annealing at 400°C is studied by X-ray resonant magnetic reflectivity (XRMR) in the soft X-ray range. Analysis of the angular dependence of the magnetic asymmetry reveals a perpendicular magnetization gradient with a significant increase in Fe and Co magnetization at the MgO interface and a 50% reduction at the W interface. In addition, the evolution of the magnetization profile, exposed to an external in-plane (*ip*) magnetic field, is discussed.

II. X-RAY RESONANT MAGNETIC REFLECTIVITY

XRMR is a powerful tool to probe the depth magnetization profile of a specific magnetic element in thin films, with sub-nanometer spatial resolution [6,7]. It exploits the dependence of the atomic scattering factor (ASF) with respect to the scattering vector q, incident photon energy, the polarization state of the incident and reflected beam as well as amplitude and orientation of the magnetization [8]. When the X-ray photon energy is tuned to an absorption edge of a magnetic element, the energy-dependent correction terms $f'(E)+if''(E)$ to the Thomson scattering $f_0(q)$ and energy-dependent magnetism-sensitive scattering term $f_m(E) = m'(E)+im''(E)$ can be enhanced. The effect is particularly strong at the L_{23} edges of 3d element in the soft X-ray range, where it is possible to use X-ray circular magnetic dichroism (XMCD) effects [9]. In addition, thanks to the longer wavelength, angle-dependent specular reflectivity can be measured up to large scattering angles, providing sensitivity to *oop* magnetization [10,11].

The XRMR measurements are performed at room temperature using the RESOXS end station [12] at SEXTANTS beamline [13] at Synchrotron SOLEIL (France). The current magnetization device allows the application of a magnetic field in all directions of the sample plane but not perpendicular to the sample. Therefore, only thin films exhibiting 100% *oop* spontaneous magnetization can be investigated. The magnetic contrast is derived from the measurement of two intensities I_p and I_m, obtained either by using right and left circularly polarized incident light, keeping the direction of the applied magnetic field unchanged or measuring at remanence, or by reversing the direction of an applied magnetic field while keeping the X-ray helicity unchanged. The magnetic asymmetry is defined as $R = [(I_p–I_m)/(I_p+I_m)]$. The sample is first magnetized by a permanent perpendicular magnet of $\mu_o H$ = 0.4 T brought close to the sample surface followed by measurements at remanence [11] and, second, is subjected to an *ip* magnetic field of 0.17 T (maximum *ip* field currently available) at the intersection of the diffraction plane and the sample plane.

III. RESULTS AND DISCUSSION

We study here a half magnetic tunnel junction [MgO(~1)/$Co_8Fe_{72}B_{20}$(1.6)/W (2)/Ta (1)/Pt (3)], part of a series of samples prepared with Ta and W/Ta cap layers of different thicknesses (nominal thickness in nm). They are deposited on [Si/SiOx//Ta (3)/CoFeB (0.4)]. Details on the preparation of the stack are given in [3]. Figure 1 shows the hysteresis loops obtained by Extraordinary Hall Effects for the perpendicular magnetic field, where the signal is proportional to the perpendicular component of the magnetization, and by SQUID for the parallel magnetic field. All measurements were performed at 300K and 1T. The $M(H_{perp})$ curve shows that 100% of the saturation magnetization (M_s) can be maintained at the zero field. The shape of the $M(H_{par})$ curve indicates that before saturation, a canted magnetic configuration could appear [14]. M_s = 1500±125 emu/cm^3 is properly determined after a calibration using a Fe sample of similar size and the same parameters for the magnetic measurements and by considering the actual rather than nominal thickness of CoFeB.

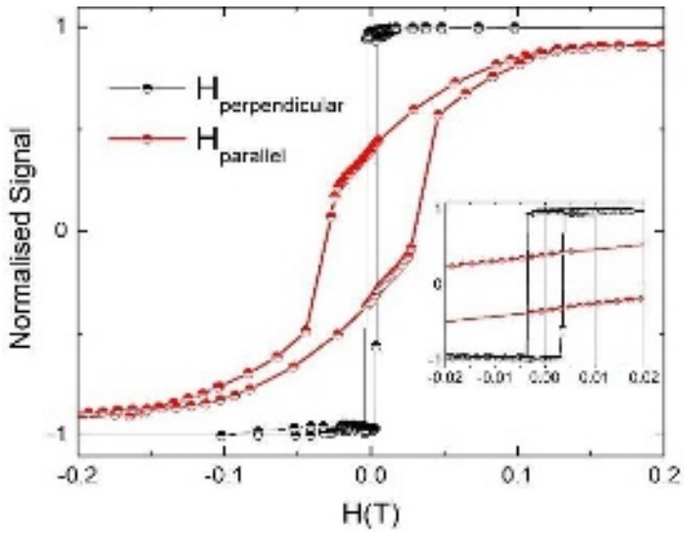

FIG. 1. Normalized magnetic loops at room temperature for perpendicular and planar magnetic fields. Inset shows a close-up of the small magnetic field region.

The study of the magnetization profile relies on the refinement of *R*, derived from angle-dependent reflectivity, which requires the determination of the structural parameters of the heterostructure. In order to allow a more unequivocal analysis of the X-ray reflectivity [15], the data are collected at various incident photon energies 670 eV and 760 eV, far from both the Fe L_3 (706.8 eV) and Co L_3 (778.1 eV) edges and at a few energies close to the edges. Figure 2 shows the non-magnetic intensities $I_{ave} = (I_p + I_m)/2$ and the fitting curves as a function of the scattering vector q for energies close to the Fe L_3 edge. The variations in the shape of the intensities are linked to the energy dependence of $f_1 = Z+f'$ ($f_0 \approx$ Z in the soft X-ray range) and $f_2 = f''$ for Fe in $Co_8Fe_{72}B_{20}$ (shown in the inset). They are well reproduced (also at the edge Co), leading to consistent parameters. The density (ρ in mol/cm^3), thickness (t in nm) and the interfacial roughness (σ in nm) for the main layers are listed here: Pt (0.091±0.003 / 2.92±0.24 / 0.24±0.01), Ta (0.083±0.004 / 1.09±0.18 / 0.56±0.2), W (0.089±0.005 / 1.93±0.24 / 0.29±0.19), CoFeB (0.129±0.015 / 1.36±0.10 / 0.5±0.04) and MgO (0.159±0.017 / 1.36±0.08 / 0.31±0.02).

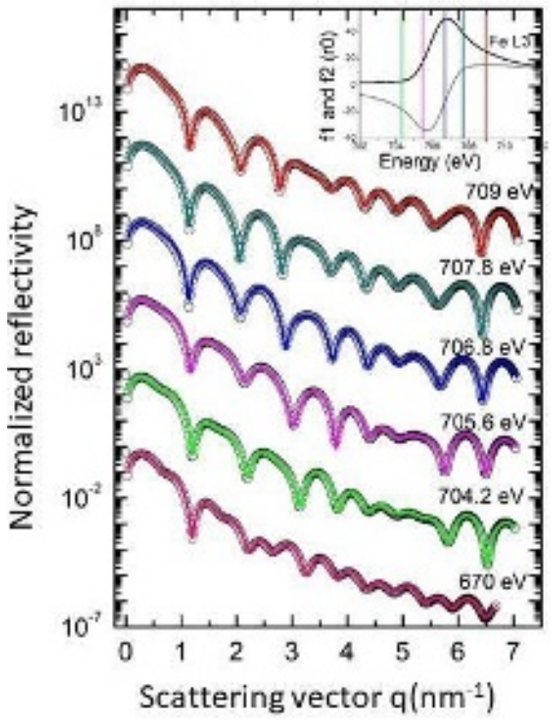

FIG. 2. X-ray reflectivity data (open circles) for energies near the Fe L3 edge (inset) and at 670 eV with limited resonant effects. The curves are shifted vertically for the sake of clarity and the best fits are plotted in continuous lines.

We now turn to the analysis of the *R* measured in the remnant condition. The reflectivity curves are collected up to an incident angle of 80° corresponding to $q_{max} \approx 7$ nm^{-1} at the Fe L_3 edge. The dichroic effect in I_p and I_m is illustrated in Figure 3a for 706.8 eV. Together with the absence of splitting at low angles, a clear splitting at larger angles is a strong indication of a net perpendicular magnetization, as expected. Such features are present in the data for all the energies at both edges. Figure 3(b, c, d) displays the *q*-dependence of *R* derived at 706.8 eV, 709 eV and at 778.1 eV. They exhibit changes related to *m'*(E) and *m"*(E) (not shown) that are derived from reference samples [16]. The refinement is performed by considering an increasing number of sub-layers in CoFeB and by adjusting for each one a weighting factor ω, modifying the f_m(E) amplitude and the thickness, while the other structural parameters are kept fixed. This corresponds to modifying the magnetization, averaged laterally over a certain thickness across the layer. Its amplitude is linked to the XMCD of the reference samples. A value ω = 1 implies an amplitude of the 3*d* magnetic moment of 2.1 μ_B for Fe and 1.7 μ_B for Co, which results from the application of the sum rules [16]. A homogeneous *oop* magnetization profile across the CoFeB layer did not permit to fit the data and a minimum of four sub-layers was required to get the best fits at all energies, as illustrated in Fig. 3. The adjustment is constrained by simultaneously refining *R* and I_{ave}. The CoFeB layer exhibits an *oop* magnetization gradient as depicted by the ω changes from 1.16±0.13 at the MgO/CoFeB interface to 0.52±0.17 at the CoFeB/W one, in the inset of Fig. 3a for Fe and similar for Co (Fig. 3d). This corresponds to a gradual decrease of 2.4±0.3 μ_B to 1.1±0.4 μ_B. Another depth profile model, based on a dead layer 0.6 nm thick [3,4] at the upper interface and homogeneous magnetization over the rest of the layer, was tested and cannot reproduce the data over the entire angular range (Fig. 3b).

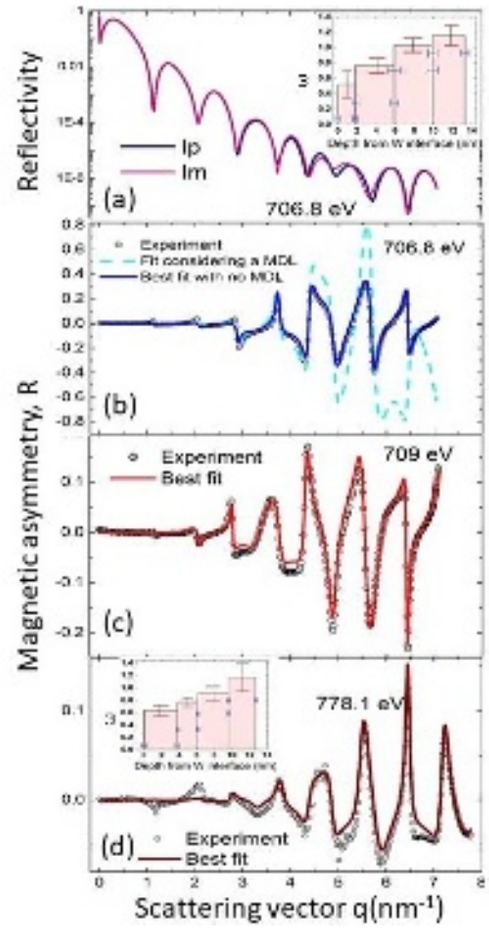

FIG. 3. Reflectivity curves for circular right and left polarized incident beam(a). Magnetic asymmetries for three resonant energies and their best fits (b, c, d). For 706.8 eV, a model with a dead layer is shown in a dashed line for comparison.

We finally present the study of the magnetization profile under a 0.17 T *ip* magnetic field applied parallel to the diffraction plane. Referring to the parallel hysteresis loop (Fig. 1), this value is insufficient to saturate the magnetization but appears sufficient to achieve a single domain configuration. Figure 4a shows I_p and I_m reflectivity curves at 706.8 eV that now exhibit a splitting at low angles indicating the presence of a net *ip* magnetization component. At the same time, a net *oop* contribution persists as can be seen at larger angles in the 706.8 eV and 709 eV magnetic asymmetries (Figures 4b and 4c). This behavior was observed for the five Fe resonant energies (no data at the Co L_3 edge). This is in agreement with a canted configuration [17]. The fits of *R* lead to a similar magnetization gradient (inset) with a tilt angle of $\varphi = 34\pm3$ degrees for the four sub-layers. We did not try to probe the distribution of tilt angles across the layer [18] since a constant value for a 1.36 nm thick layer provides a very good fit for the data.

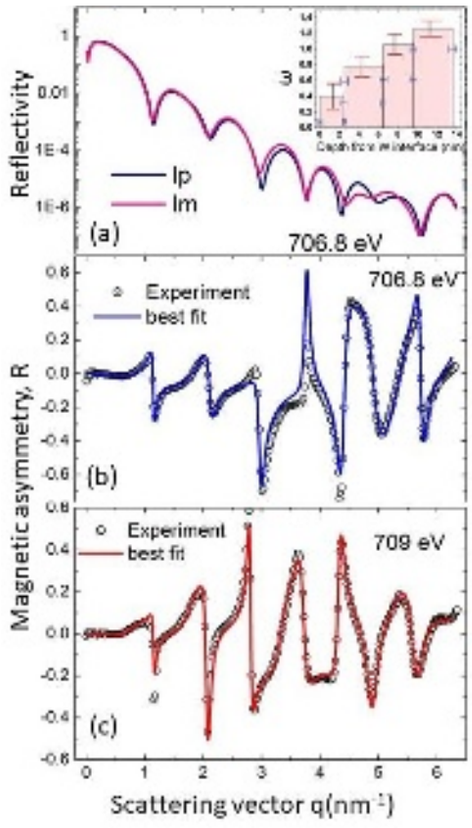

FIG. 4. Reflectivity for circular right and left polarized incident beam with H_{par} = 0.17 T(a). Magnetic asymmetries for two resonant energies and their best fits (b, c).

IV. CONCLUSION

A first notable characteristic of the Fe magnetization profile within the annealed CoFeB layer is a high 3*d* magnetization in the first 0.3±0.09 nm thick sublayers (about 2 ML) at the MgO interface. Such an enhancement of the magnetization has also been observed for Fe on MgO studied by XMCD [19] and for Fe in the 2–3 ML near both MgO interfaces in a MgO/Fe (12 nm)/MgO (001) trilayer by using SXRMR [20] and theoretically discussed [21]. We found a similar magnetization increase for Co. A second feature is the lowering in magnetization towards the W interface, which is more pronounced after 0.7 nm from the MgO interface (thickness of the two sublayers). This decrease is ascribed to a localized reduction of M_S and T_C due to alloying of CoFeB with W, as proposed earlier [22]. This is supported by a 0.5 nm roughness at the CoFeB/W interface. The averaged ω value from the Fe magnetization profile amounts to 0.91±0.13, corresponding to 1.9±0.3 μ_B, which leads to 1480±234 emu/cm^3 in reasonably good agreement with the value derived from SQUID data. We also characterize the magnetization profile for various values of the applied magnetic field from 0.17 T to 0.02 T. The modification concerns mainly the tilt angle that varies linearly from 34 to 4 degrees, indicating the magnetization gradient is a robust property of the CoFeB layer in the investigated sample.

This investigation is part of a larger investigation dedicated to the comparison of the magnetization profile between as-deposited samples and annealed samples with a Ta (1 nm) cap layer and a W (2 nm)/Ta (1 nm) cap layer. The full results will be published elsewhere.

V. ACKNOWLEDGMENTS

Financial support from the Agence Nationale de la Recherche, France, under Grant Agreement No. ANR-16-CE09-0009 (WAVENEXT) is acknowledged.

VI. REFERENCES

[1] H. Ohno, T. Endoh, T. Hanyu, N. Kasai, and S. Ikeda, "Magnetic tunnel junction for nonvolatile CMOS logic," in Proc. IDTM Tech. Dig., 218-221 (2010)
[2] S. Ikeda, K. Miura, H. Yamamoto, K. Mizunuma, H.D. Gan, M. Endo, S. Kanai, J. Hayakawa, F. Matsukura, H. Ohno, Nat. Mater. **9**, 721 (2010)
[3] J. Chatterjee, R. C. Sousa, N. Perrissin, S. Auffret, C. Ducruet, and B. Dieny, Appl. Phys. Lett. **110**, 202401 (2017)
[4] J. Chatterjee, E. Gautier, M. Veillerot, R.C. Sousa, S. Auffret, and Bernard Dieny, Appl. Phys. Lett. **114**, 092407 (2019)
[5] J. Z. Sun, Phys. Rev. B **91**, 174429 (2015)
[6] J.M. Tonnerre, E. Jal, E. Bontempi, N. Jaouen, M. Elzo, S. Grenier, H.L. Meyerheim and M. Przybylski, Eur. Phys. J. Special Topics **208**, 177 (2012)
[7] S. Macke and E. Goering, J. Phys.: Condens. Matter **26**, 363201, 15-17 (2014)
[8] J. P. Hill and D. F. McMorrow, Acta Crystallogr. Sect. A **52**, 2, 236-244 (1996)
[9] J. Stöhr, J. Magn. & Magn. Mat. **200**, 1, 470-497 (1999)
[10] J.-M. Tonnerre, M. De Santis, S. Grenier, H. C. N. Tolentino, V. Langlais, E. Bontempi, M.Garcıa-Fernandez, and U. Staub, Phys. Rev. Lett. **100**, 157202 (2008)
[11] H. L. Meyerheim, J.-M. Tonnerre, L. Sandratskii, H. C. N. Tolentino, M. Przybylski, Y. Gabi, F. Yildiz, X. L. Fu, E. Bontempi, S. Grenier, and J. Kirschner, Phys. Rev. Lett. **103**, 267202 (2009)
[12] N. Jaouen, J.-M. Tonnerre, G. Kapoujian, P. Taunier, J.-P. Roux, D. Raoux and F. Sirotti, J. Synchrotron Rad. **11**, 353-357 (2004)
[13] M. Sacchi, N. Jaouen, H. Popescu, R. Gaudemer, J.-M. Tonnerre, S.G. Chiuzbaian, C.F. Hague, A Delmotte, J.-M. Dubuisson and G. Cauchon, J. Phys.: Conf. Series **425**, 072018, 6-10 (2013)
[14] B. Dieny and A. Vedyavev, Eur. Phys. Lett. **25**, 723-728 (1994)
[15] N. Jaouen, J.-M. Tonnerre, D. Raoux, E. Bontempi, L. Ortega, M. Müenzenberg, W. Felsch, A. Rogalev, H.A. Dürr, E. Dudzik, G. van der Laan, H. Maruyama and M. Susuki, Phys. Rev. B **66**, 134420 (2002)
[16] C.T. Chen, Y.U. Idzerda, H.-J. Lin, H. Smith, G. Meigs, E. Chaban, G. Ho, E. Pellegrin, F. Sette, Phys. Rev. Lett. **75**, 152 (1995)
[17] J.-M. Tonnerre, M. Przybylski, M. Ragheb, F. Yildiz, H. C. N. Tolentino, L. Ortega, and J. Kirschner, Phys. Rev. B **84**, 100407 (2011)
[18] T. Kawauchi, Y. Miura, X. Zhang, and K. Fukutani, Phys. Rev. B **95**, 014432 (2017)
[19] K. Miyokawa, S. Saito, T. Katayama, T. Saito, T. Kamino, K. Hanashima, Y. Suzuki, K. Mamiya, T. Koide, and S. Yuasa, Jpn. J. Appl. Phys., Part 2 **44**, L9 (2005)
[20] E. Jal, J.B. Kortright, T. Chase, T.M. Liu, A. X. Gray, P. Shafer, E. Arenholz, P. Xu, J. Jeong, M. G. Samant, S.S. P. Parkin, and H. A. Dürr, Appl. Phys. Lett. **107**, 092404 (2015)
[21] J.I. Beltrán, Lluis Balcells and C. Martínez - Boubeta, Phys. Rev. B **85**, 64417 (2012)
[22] B. M. S. Teixeira, A. A. Timopheev, N. Caçoilo, S. Auffret, R. C. Sousa, B. Dieny, and N.

Sobolev, Phys. Rev. B **100**, 184405 (2019)

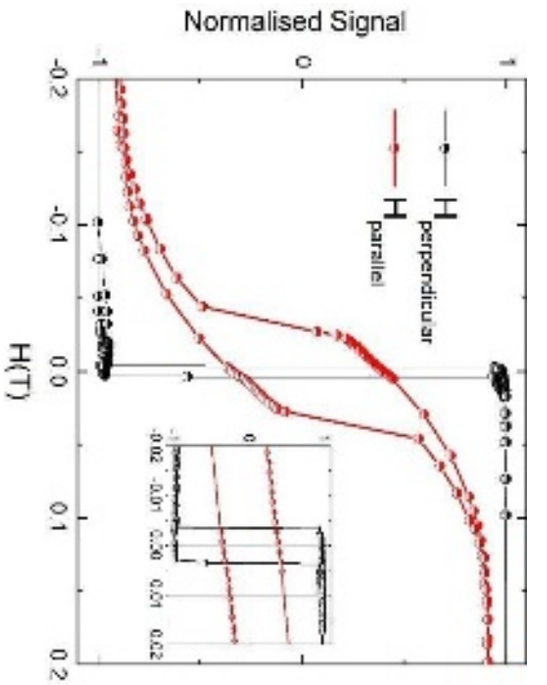

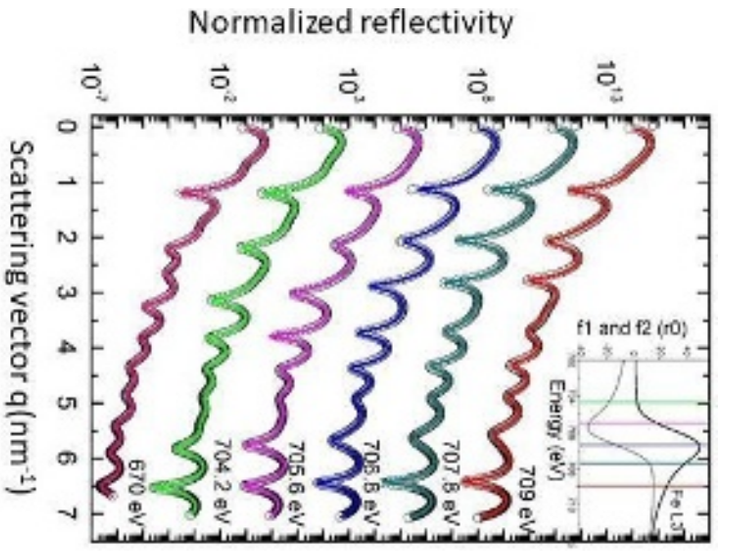

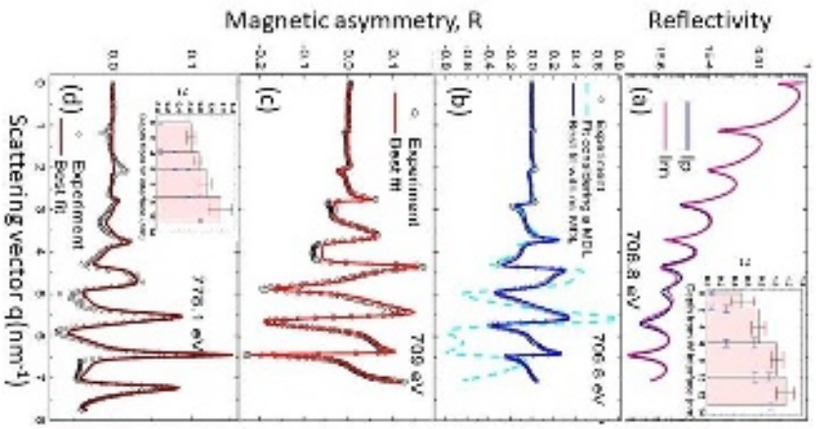

PLEASE CITE THIS ARTICLE AS DOI: 10.1063/9.0000343